3rd Huixian International Forum on Earthquake Engineering for Young Researchers
August 11-12, 2017, University of Illinois, Urbana-Champaign, United States

Development of Bidirectional Cyclic Lateral Loading Protocols for Experimental Testing of Steel Wide-Flange Columns

A. Elkady[1], and D.G. Lignos[2]

1 *Postdoctoral Research Scientist, Resilient Steel Structures Laboratory (RESSLab), Swiss Federal Institute of Technology i Lausanne (EPFL), Switzerland.*
E-mail: ahmed.elkady@epfl.ch

2 *Associate Professor, Resilient Steel Structures Laboratory (RESSLab), Swiss Federal Institute of Technology in Lausanne (EPFL), Switzerland.*
E-mail: dimitrios.lignos@epfl.ch.

ABSTRACT
Steel columns in frame buildings subjected to earthquake shaking undergo bidirectional lateral drift demands. Till now, the majority of past experimental and numerical studies were primarily concerned with the unidirectional column behavior. This paper proposes a procedure to develop representative bidirectional lateral drift histories for experimental testing of steel columns in moment-resisting frames (MRFs). To this end, a 3-dimensional numerical model of a prototype four-story building with perimeter MRFs is analyzed using a suite of ordinary ground-motion records. The first-story drift orbit is idealized in the form of elliptical drift cycles. Statistical data of parameters defining these elliptical drift cycles is collected. The data serves for the development of bidirectional symmetric loading protocols representative of design-basis earthquakes. The developed protocol is adopted in a testing program that assessed in full-scale the influence of bidirectional cyclic loading on steel columns.

KEYWORDS: *Loading protocol, bidirectional drift, biaxial bending, steel columns, full-scale testing.*

1. INTRODUCTION

During an earthquake, columns in steel-frame buildings experience bidirectional lateral drift demands due to the two horizontal components of the ground-motion shaking. During design-basis earthquakes, steel-frame buildings with conventional lateral load resisting systems and symmetric plan views move in a 45° orientation (MacRae and Tagawa 2001; Suita et al. 2008; Palmer et al. 2013); therefore, their columns experience balanced biaxial bending. Shake table tests that examined the collapse behavior of steel-frame buildings (Suita et al. 2008) indicated that at large deformations, damage progresses in the column's strong-axis direction; the building tends to displace more in this loading direction rather than the orthogonal one (i.e. ratcheting behavior).

The majority of past experimental studies focused on the cyclic behavior of steel columns under strong or weak axis bending. This is mainly attributed to the complexity and equipment limitations associated with bidirectional testing as well as the absence of protocols representative of steel columns' bidirectional lateral drift demands. Referring to Fig. 1.1a, Ishida et al. (2012), Chen et al. (2014) and Ozkula et al. (2017) utilized simplified linearly-proportional bidirectional protocols in which the column was pushed with a constant loading angle (Ψ) with respect to its strong-axis. A more robust protocol was developed and utilized by Ishida et al. (2013) after analyzing random horizontal drift orbits obtained through elasto-plastic response-history analyses of multi-story steel-frame buildings subjected to 3-dimensional shaking. Referring to Fig. 1.1b, this protocol consists of a set of three ellipses with increasing amplitude and a shifting major-axis with a loading angle (Ψ) equal to -30°, 0 °, +30°. Others (Bousias et al. 1995; Watanabe et al. 2000; Goto et al. 2006; Ucak and Tsopelas 2015) utilized bidirectional out-of-phase lateral loading paths (ex. square-, diamond-, and circular-shaped paths) as shown in Fig. 1.1c.

The above protocols were mainly developed in a qualitative manner and in many cases were only case-specific. This paper outlines a quantitative methodology to develop representative bidirectional protocols for experimental testing of steel columns subjected to cyclic loading. For this purpose, a prototype four-story office steel-frame building with perimeter MRFs is analyzed under 3-dimensional ground motion shaking. The focus is on first-story steel columns in which plastic deformations are allowed at their base based on capacity-design principles. The proposed protocol is utilized in full-scale experiments of deep wide-flange steel columns subjected to multi-axis cyclic loading.

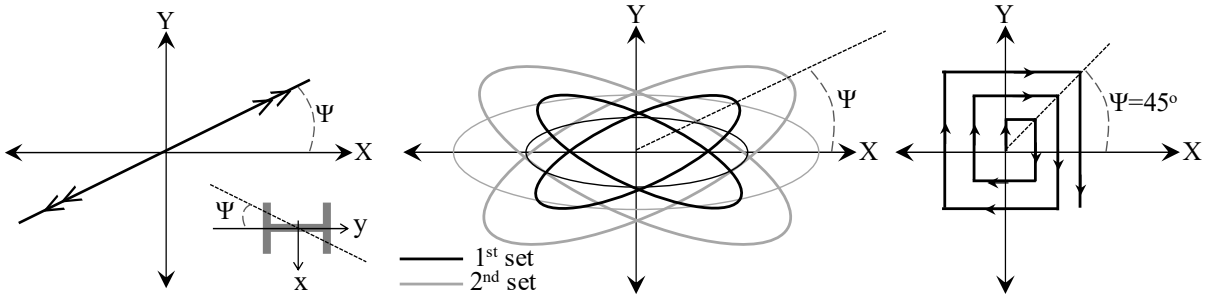

(a) Linearly proportional (b) Elliptical cycles (Ishida et al. 2013) (c) square-shaped

Figure 1.1 Typical bidirectional loading protocols

2. PROTOTYPE STEEL-FRAME BUILDING AND GROUND-MOTION RECORDS

A 3-dimensional (3D) numerical model of a prototype four-story archetype steel frame building, with perimeter 3-bay MRFs and reduced beam-section connections, is modeled and analyzed in the OpenSees platform (Mckenna 1997). Referring to Fig. 2.1a, the building is symmetric in plan view located in downtown Los Angeles, California, in a site Class D. The design details of the MRFs as well as the gravity framing system can be found in (Elkady and Lignos 2014, 2015). All members are modeled with force-based nonlinear beam-column elements. The wide-flange cross-sections are discretized with fiber elements. The fiber elements are assigned the Menegotto and Pinto (1973) material model that simulates the combined kinematic and isotropic hardening of a steel material. The steel MRF columns are assumed to be fixed at the ground level. A rigid diaphragm is assumed at each floor. P-Delta effects are explicitly simulated. The first and second mode periods of the model in the EW and NS directions are T_1=1.27sec and T_2=1.24sec, respectively.

The Pacific Earthquake Engineering Research Center (PEER) ground-motion selection web application (PEER 2013) is utilized in order to select and scale a suite of records that match the design spectrum of the building site. The selection criteria were based on a magnitude M_w ranging from 6.0 to 8.0 and a source-to-site distance R ranging from 5 to 20 km. These ranges represent earthquakes contributing the most to the seismic hazard, based on deaggregation data (USGS 2014). A set of 53 records was assembled. The records were scaled to match the design spectrum (corresponding to 10% probability of exceedance in 50 years) between the period range of 0.2 T_1 and 3 T_1 (Eads et al. 2015), as shown in Fig. 2.1b.

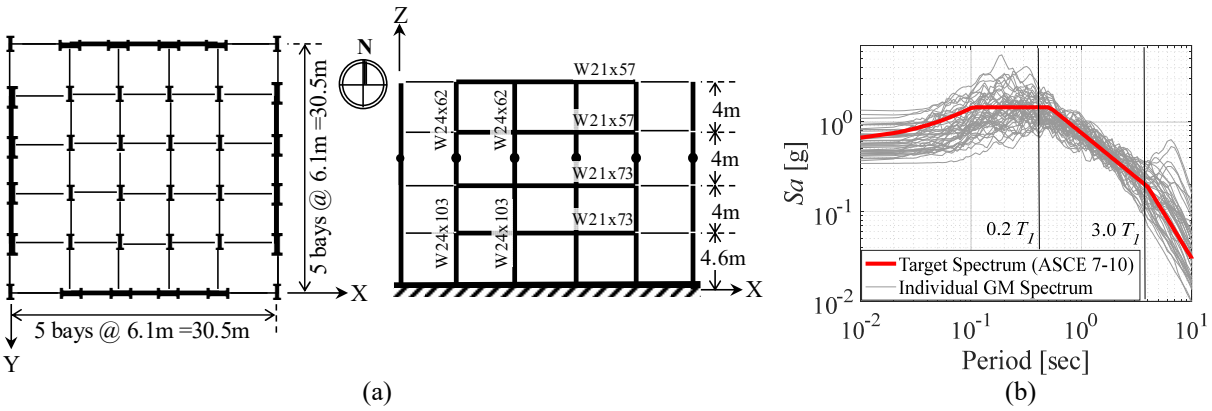

(a) (b)

Figure 2.1 (a) Plan view and elevation of the prototype 4-story building; (b) target response spectrum and scaled ground motion acceleration response spectra

Nonlinear response-history analyses (NRHA) are conducted with the 53 records scaled to the design-basis seismic intensity. For each record, the stronger of the two horizontal components (i.e., the component that yields the largest drift) is applied to the building's global X- direction, while the orthogonal horizontal component is assigned to the Y-direction. Similarly, the vertical component of the ground motion is assigned to the Z-direction. Therefore, the angle of incidence between the ground motion and the building principle axis is either 0° or 90°. Giannopoulos and Vamvatsikos (2015) illustrated that the ground-motion component rotation with respect to the building does not practically affect the seismic behavior of frame buildings. Instead, one should invest into selecting more

ground motion records to conduct nonlinear response history analysis because the record-to-record variability is more influential on the seismic behavior of frame buildings. Rayleigh damping is incorporated in the 3D model. Two percent damping ratio (ζ=2%) is assumed at the first and sixth mode.

3. COLUMN DRIFT ORBIT PROCESSING

Past studies related to the development of lateral loading protocols (Clark et al. 1997; Krawinkler et al. 2001; Richards and Uang 2006) utilized the "Rainflow" method (Matsuishi and Endo 1968) to process the drift response-history and obtain the drift-cycle data. This data was utilized to define a loading protocol in term of the number, range/amplitude, and sequence of occurrence of the respective drift cycles. However, to fully define a bidirectional protocol in the form of elliptical drift cycles, additional parameters should be considered. These include the drift range/amplitude in the orthogonal direction (i.e., weak-axis direction), the elliptical cycle's major-axis angle, and the elliptical cycle's "*ellipsity*" (i.e., ratio of minor-to-major axis length). In this case, the Rainflow counting method cannot be employed. This method can only deal with a single unidirectional drift-history at a time.

To obtain the statistical data required to develop a bidirectional loading protocol, the first-story drift-ratio histories in the X- versus the Y-direction (i.e., *SDR* orbit) are deduced for each one of the 53 records. Figure 3.1a shows a sample *SDR* orbit based on the "EC County Center FF" record from the 1979 Imperial Valley earthquake. Referring to Fig. 3.1, the elliptical-shaped drift cycles represent well the column orbit during the ground-motion shaking. The *SDR* orbit is processed in order to identify the complete "XY drift cycles". To this end, the drift history is first discretized by filtering out all the drift points other than the vertex drift points. A second filter is applied to remove all the drift excursions with a range less than 0.1%. Figure 3.1b shows the discretized and filtered *SDR* orbit. A complete XY drift cycle is then defined as any drift excursion that starts at a given drift peak/valley point in the X-direction, reaches the next peak/valley point in the X-direction, and then returns to the starting drift in the same direction. A complete XY drift cycle has a sequence of peak-valley-peak or valley-peak-valley in the X-direction. Referring to Fig. 3.1c, some of the loading cycles, identified for the same ground motion record, are highlighted with different colors.

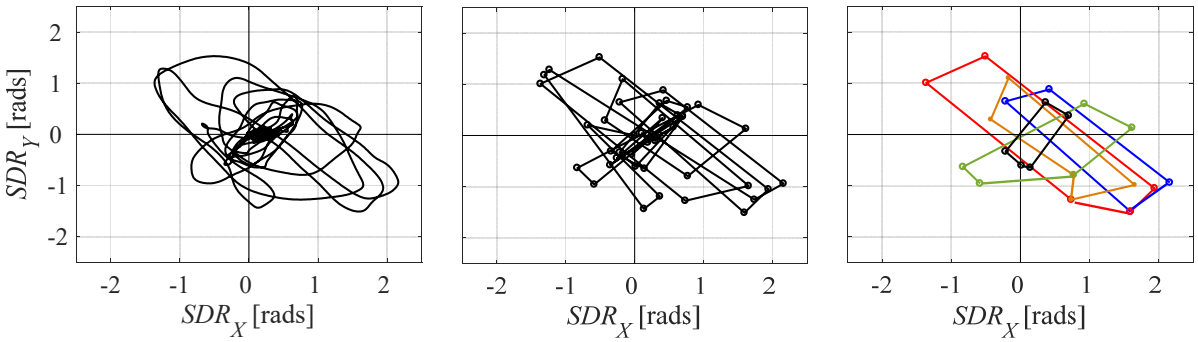

(a) Original orbit (b) discretized and filtered orbit (c) identified cycles

Figure 3.1 Illustration of the discretization, filtering, and cycle identification for a typical *SDR* orbit

A number of parameters are utilized to approximate the identified cycles into elliptical ones as illustrated in Fig. 3.2 including: (a) the offset of the drift cycle center in the X- and Y-directions from the undeformed configuration (X_{offset} and Y_{offset}, respectively); (b) the length of the straight line joining the peak drift points in both the X- and Y-directions (L_X and L_Y, respectively); and (c) the angle between the straight line joining the peak drift points in both the X- and Y-directions and the X-axis (Ψ_X and Ψ_Y, respectively). An elliptical cycle can be defined using three parameters:

1) The cycle's *SDR* amplitude in the X-direction (SDR_X); note that the SDR_X amplitude is half of the SDR_X range.
2) The cycle's *ellipsity*, defined as the minor-axis to major-axis length ratio of the elliptical cycle. This parameter is calculated using Eq. 3.1.
3) The cycle's major-axis angle (Ψ_{major}) with respect to X-axis; note that the elliptical cycle has four possible orientations as shown in Fig. 3.2. The major-axis angle, Ψ_{major}, is evaluated based on a weighting scheme given by Eq. 3.2 that includes the two characteristic angles of the XY drift cycle; Ψ_Y, and Ψ_X,

$$ellipsity = \begin{cases} L_Y \cos(90 + \psi_X - \psi_Y)/L_X & \text{if } L_X \geq L_Y \\ L_X \sin(\psi_Y - \psi_X)/L_Y & \text{if } L_Y > L_X \end{cases} \tag{3.1}$$

$$\psi_{major} = \frac{\psi_X L_X + \psi_Y L_Y}{L_X + L_Y} \tag{3.2}$$

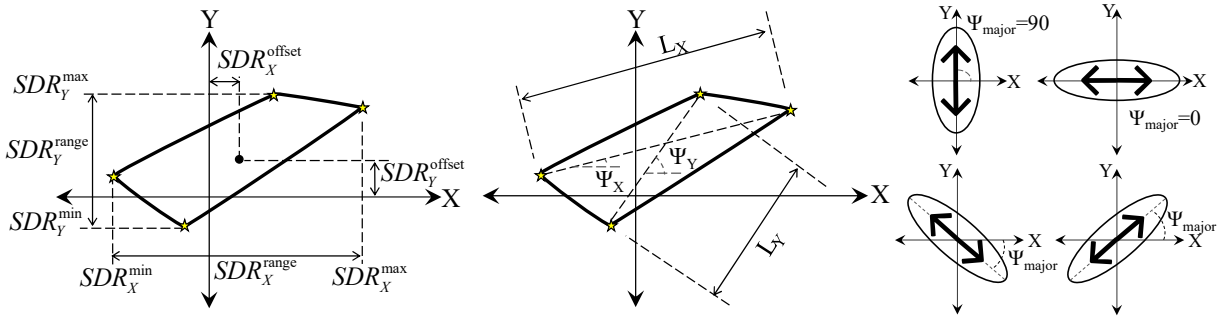

Figure 3.2 Illustration of parameters defining the XY drift cycles

Figure 3.3 shows summary plots for the aforementioned cycle parameters. Referring to Fig. 3.3a, at SDR_X up to 0.75%, the SDR_Y-to-SDR_X ratio is approximately equal to one; implying balanced biaxial column bending demands. This ratio decreases while the SDR_X amplitudes increase. Note that the maximum SDR_Y was 1.4% when SDR_X reached 2% from NRHA. Note that the prototype steel-frame building was designed for a maximum allowable *SDR* of 2.5% according to ASCE (2010). Referring to Fig. 3.3a, the number of loading cycles decreases at higher amplitudes. This is consistent with the unidirectional AISC symmetric-cyclic protocol (Clark et al. 1997). Referring to Fig. 3.3b, the offset of the cycle's center is clustered around 0% rads in both loading directions. This is expected at a design-basis seismic intensity, because steel columns exhibit minor flexural yielding. In this case, minor residual *SDR* is likely to develop. Note that some loading cycles have a relatively large offset; these are mainly associated with low *SDR* amplitudes. Figures 3.3c and 3.3d suggest that that the cycle's major-axis angle and ellipsity decreases while the SDR_X amplitudes increase. In average, the cycles start with Ψ of 60° and *ellipsity* of 0.6 and reduce to Ψ of 25° and *ellipsity* of 0.2 at an SDR_X amplitude of 2%.

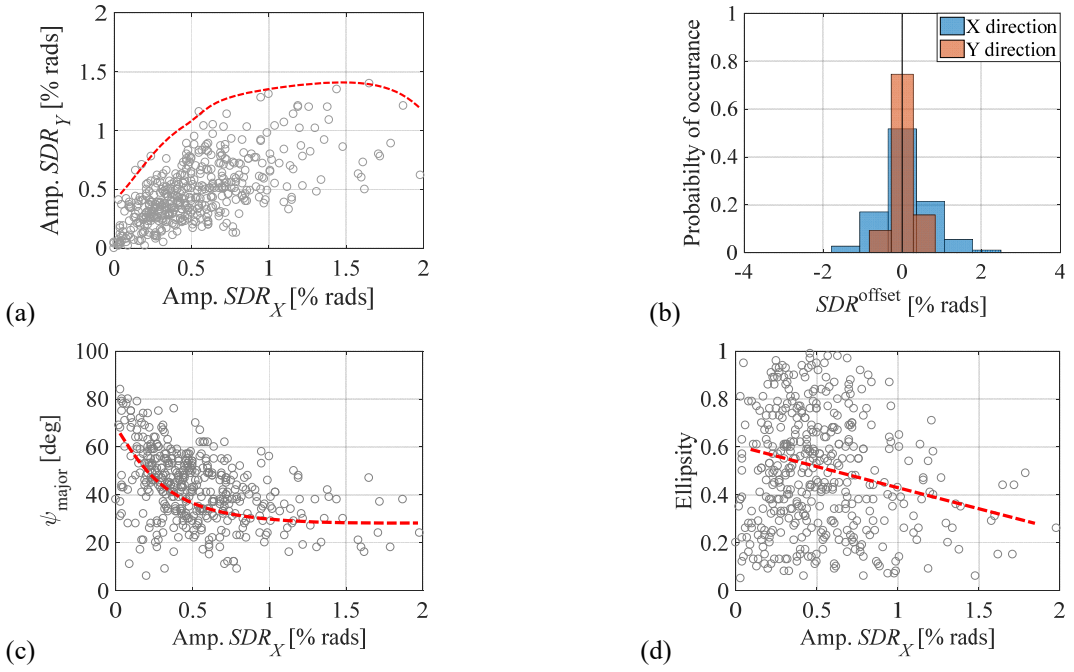

Figure 3.3 (a) SDR_Y versus SDR_X amplitudes; (b) histogram of the cycle offset in both orthogonal directions; (c) major-axis angle versus SDR_X amplitude; (d) cycle ellipsity versus SDR_X amplitude

Table 3.1 summarizes the statistical data regarding the number of XY cycles per ground-motion record (n), major-axis angle (Ψ_{major}), and cycle *ellipsity*. For reference, these data are summarized based on discrete SDR_X bins that correspond to the peak SDR_X amplitudes of the standard unidirectional AISC protocol. Refereeing to Table 3.1,

four cycles (one in each orientation) are counted at each target SDR_X amplitudes up to 1.5% followed by two cycles at 2%. Note that the average number of complete XY drift cycle per record (n) is divided by the number records (i.e., 53) and rounded up to the nearest integer. Using the statistical data from Table 3.1, a bidirectional lateral loading protocol can be proposed. Its loading cycles are summarized in Table 3.2. From this table, the protocol is continued beyond 2% rads, where two cycles are applied at increments of 1% rads, in order to characterize the column behavior beyond this drift level. This is consistent with the AISC symmetric cyclic loading protocol; although this is an artifact, since the maximum *SDR* does not exceed 2% at design-basis earthquakes. If the objective is to characterize the collapse behavior of steel columns then loading histories that capture "ratcheting" should be employed (Lignos et al. 2009; Suzuki and Lignos 2014).

Figure 3.4a shows the XY drift history of the developed bidirectional protocol, up to an SDR_X of 4%. Referring to Fig. 3.4b, the sequence of the four elliptical cycles at an SDR_X amplitude of 1% is demonstrated. In summary, the developed bidirectional symmetric lateral loading protocol reaches a maximum *SDR* in the Y-direction (i.e., the column's weak-axis) of 2% during the 3% drift cycle in the X-direction. The loading angle of the elliptical cycles with respect to the X-direction starts at 50° at 0.375% rads and reduces to 35° at 2% rads. Beyond this amplitude, the cycle ellipsity is kept constant at 0.2 while the major-axis angle is reduced gradually until it reaches 0° at SDR_X of 5%.

Table 3.1 Summary statistical data for the XY drift cycles at design-basis intensity

Parameter	Orient.	Target SDR_X Amplitudes [% rads]					
		0.375	0.50	0.75	1.0	1.5	2.0
n-Ψ_{major}-*ellipsity*	→	1-00-0.67	1-00-0.73	1-00-0.73	1-00-0.82	1-00-0.83	-
	↑	1-90-0.78	1-90-0.77	1-90-0.70	1-90-0.70	1-90-0.64	-
	↗	1-50-0.47	1-49-0.31	1-45-0.40	1-43-0.41	1-38-0.33	1-37-0.38
	↖	1-47-0.50	1-44-0.52	1-44-0.48	1-43-0.43	1-38-0.27	1-38-0.15

Table 3.2 Steps of the proposed bidirectional symmetric protocol

Parameter	Orient.	Target SDR_X Amplitudes [% rads]								
		0.375	0.50	0.75	1.0	1.5	2.0	3.0	4.0	+1.0
n-Ψ_{major}-*ellipsity*	→	1-00-0.8	1-00-0.8	1-00-0.7	1-00-0.7	1-00-0.7	-	-	-	-
	↑	1-90-0.8	1-90-0.8	1-90-0.7	1-90-0.7	1-90-0.7	-	-	-	-
	↗	1-50-0.5	1-45-0.5	1-45-0.5	1-45-0.4	1-40-0.3	1-35-0.3	1-20-0.2	1-10-0.2	1-0-0.2
	↖	1-50-0.5	1-45-0.5	1-45-0.5	1-45-0.4	1-40-0.3	1-35-0.3	1-20-0.2	1-10-0.2	1-0-0.2

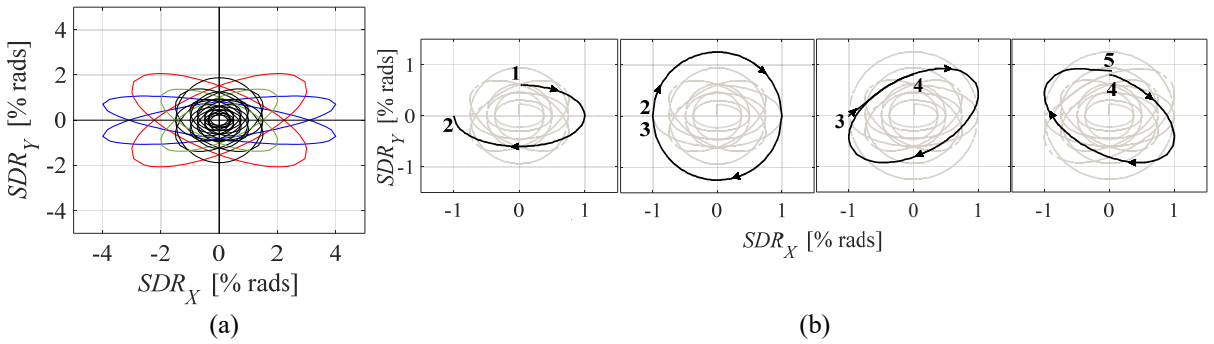

Figure 3.4 Proposed bidirectional symmetric protocol: (a) drift history up to 4% rads; (b) application sequence of the four cycles at 1% rads

4. STEEL COLUMNS UNDER BIDIRECTIONAL LATERAL LOADING

The developed protocol was incorporated in a recent full-scale testing program that investigated the hysteretic behavior of steel wide-flange columns (Elkady and Lignos 2016, 2017). The column specimens were 3.9m long (≈13ft) and utilized seismically compact W24 cross-sections. The specimens were fixed at their column base and flexible at their top end in the strong-axis direction. Fixed end boundaries were considered in the weak-axis direction. The specimens were subjected to a constant compressive axial load ratio, P/P_y = 20% (P_y is the axial yield strength). Referring to Fig. 4.1, the hysteretic behavior of nominally identical W24x84 columns is compared in terms of their deduced moment-drift relation, axial shortening-drift, and out-of-plane global deformation

profile.

From Figure 4.1a, for SDR_X larger than 3%, the rate of cyclic deterioration in flexural strength of a column is slightly larger under bidirectional loading compared to unidirectional loading. This is attributed to the additional flexural demands in the weak-axis direction of the column cross-section (i.e., P-M_x-M_y interaction). This effect is practically negligible on the maximum flexural strength of a column and on the first-cycle envelope curve of the same specimens. Same observations hold true for the column axial shortening (see Fig. 4.1b).

From Fig. 4.1a, for SDR_X larger than 3%, the unloading stiffness of a column that is subjected to bidirectional loading deteriorates much more compared to that from unidirectional loading. This is attributed to the magnitude of out-of-plane deformations near the column plastic hinge region. These deformations are more pronounced in the case of bidirectional loading. Plastic lateral torsional buckling is also more evident when the column is subjected to bidirectional loading (see Fig. 4.1c).

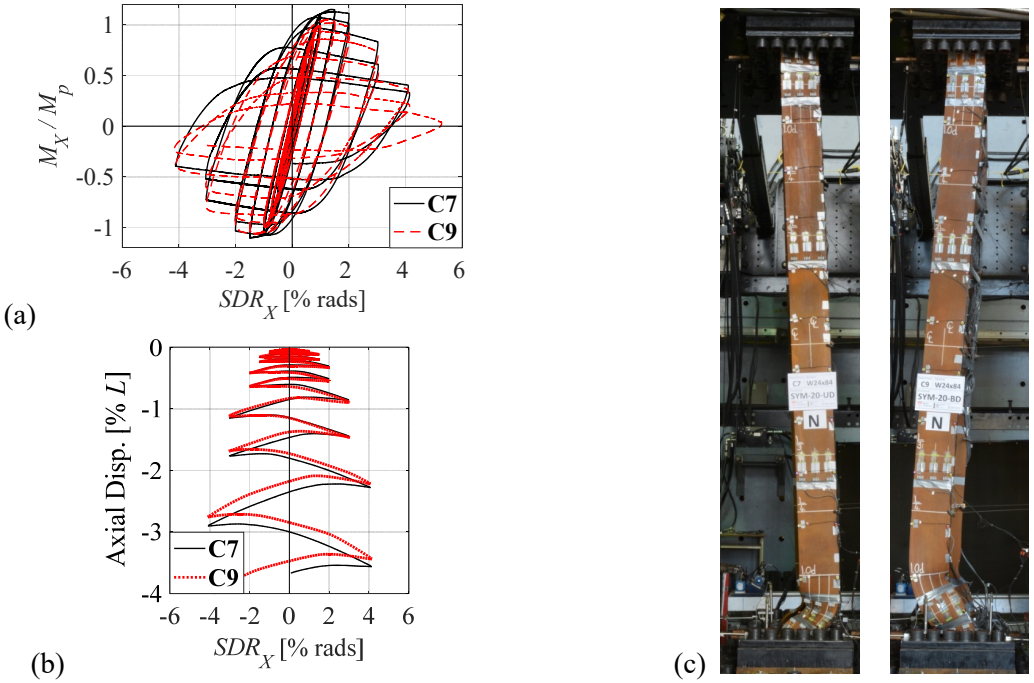

Figure 4.1. Comparison between specimens C7 and C9: (a) normalized moment-drift relation; 9b) column axial shortening-drift relation; (c) out-of-plane global deformation profile

5. SUMMARY AND CONCULUSIONS

This paper proposes a methodology to develop bidirectional lateral loading protocols based on 3-dimensional response-history analyses of a prototype four-story steel-frame building subjected to a suite of 53 ordinary ground motions. This methodology idealizes the bidirectional drift orbit of first-story columns with elliptical drift cycle sequences. Statistical data is collected regarding the number, shape, and drift amplitudes of the identified bidirectional lateral drift cycles. The statistical data is organized into discrete drift bins. Using the collected data, a bidirectional protocol is proposed. Although representative of one building, the proposed bidirectional protocol captures the drift demands that a column experiences during a design-basis earthquake with a 10% probability of occurrence in 50 years. The number of elliptical drift cycle sequences is in good agreement with the standard symmetric cyclic loading protocol up to 1.5% drift amplitude. However, the higher drift amplitude cycles are not consistent with the lateral drift demands that a steel column would experience during a design-basis seismic event.

The proposed protocol was employed in full-scale experiments that characterized the cyclic behavior of deep wide-flange columns under multi-axis cyclic loading. The results suggest that the effect of bidirectional loading on the steel column stability is significant. For the cases examined, the effect of bidirectional loading is more evident on the unloading stiffness deterioration of steel columns.

The authors are currently extending the work presented in this paper to develop bidirectional lateral loading

histories representative of low-probability of occurrence earthquakes with a 2% probability of occurrence over 50 years. The methodology presented herein is also employed to refine the proposed protocols to account for the building height as well as the steel column local slenderness.

AKCNOWLEDGEMENTS

This study is based on work supported by the Swiss National Science Foundation (SNSF Award No 200021_169248). This financial support is gratefully acknowledged. Any opinions, findings, and conclusions or recommendations expressed in this paper are those of the authors and do not necessarily reflect the views of sponsors.

REFERENCES

1. ASCE (2010). "Minimum design loads for buildings and other structures." *ASCE/SEI 7-10*, Reston, VA.
2. Bousias, S. N., Verzeletti, G., Fardis, M. N., and Gutierrez, E. (1995). Load path effects in column biaxial bending with axial force. *Journal of Engineering Mechanics*. **121:5**, 596-605.
3. Chen, Y. Y., Niu, L., and Cheng, X. (2014). Hysteretic behaviour of h steel columns with large width-thickness ratios under bi-axis moments. *Proc., 10th National Conference on Earthquake Engineering*, Anchorage, AK, USA.
4. Clark, P., Frank, K., Krawinkler, H., and Shaw, R. (1997). Protocol for fabrication, inspection, testing, and documentation of beam-column connection tests and other experimental specimens. SAC Joint Venture.
5. Eads, L., Miranda, E., and Lignos, D. G. (2015). Average spectral acceleration as an intensity measure for collapse risk assessment. *Earthquake Engineering & Structural Dynamics*. **44:12**, 2057-2073.
6. Elkady, A., and Lignos, D. G. (2014). Modeling of the composite action in fully restrained beam-to-column connections: implications in the seismic design and collapse capacity of steel special moment frames. *Earthquake Engineering & Structural Dynamic*. **43:13**, 1935-1954.
7. Elkady, A., and Lignos, D. G. (2015). Effect of gravity framing on the overstrength and collapse capacity of steel frame buildings with perimeter special moment frames. *Earthquake Engineering & Structural Dynamic*. **44:8**, 1289–1307.
8. Elkady, A., and Lignos, D. G. Dynamic stability of deep and slender wide-flange steel columns – full scale experiments. *Proc., ASCE Annual Stability Conference*, Orlando, Florida, USA.
9. Elkady, A., and Lignos, D. G. Full-scale cyclic testing of deep slender wide-flange steel beam-columns under unidirectional and bidirectional lateral drift demands. *Proc., 16th World Conference on Earthquake Engineering*, Santiago, Chile.
10. Giannopoulos, D. G., and Vamvatsikos, D. I. (2015). Influence of rotated ground motion components on the response distribution of inelastic oscillators. *Proc., 5th ECCOMAS Thematic Conference on Computational Methods in Structural Dynamics and Earthquake Engineering* Crete Island, Greece.
11. Goto, Y., Jiang, K., and Obata, M. (2006). Stability and ductility of thin-walled circular steel columns under cyclic bidirectional loading. *Journal of Structural Engineering*. **132:10**, 1621-1631.
12. Ishida, T., Shimada, Y., and Yamada, S. (2013). "Cyclic loading test on rhs columns under bi-directional horizontal forces." *10th International Conference on Urban Earthquake Engineering*Tokyo, Japan.
13. Ishida, T., Yamada, S., and Shimada, Y. Bi-axial bending behavior of rhs columns including post-buckling and deterioration range. *Proc., 15th World Conference on Earthquake Engineering*, Lisbon, Purtugal.
14. Krawinkler, H., Parisi, F., Ibarra, L., Ayoub, A., and Medina, R. (2001). Development of a testing protocol for wood frame structures. Consortium of Universities for Research in Earthquake Engineering (CUREE), Richmond, CA.
15. Lignos, D. G., Krawinkler, H., and Whittaker, A. S. Collapse assessment of a 4-story steel moment resisting frame. *Proc., Computational Methods in Structural Dynamics and Earthquake Engineering* Rhodes, Greece.
16. MacRae, G., and Tagawa, H. (2001). Seismic behavior of 3d steel moment frame with biaxial columns. *Journal of Structural Engineering*. **127:5**, 490-497.
17. Matsuishi, M., and Endo, T. (1968). Fatigue of metals subjected to varying stress. *Japan Society of Mechanical Engineers* 37-40.
18. Mckenna, F. T. (1997). "Object-oriented finite element programming: Frameworks for analysis, algorithms and parallel computing." Ph.D., University of California.
19. Menegotto, M., and Pinto, P. E. Method of analysis for cyclically loaded rc frames including changes in geometry and non-elastic behaviour of elements under combined normal force and bending. *Proc., IABSE Congress Reports of the Working Commission*.
20. Ozkula, G., Harris, J., and Uang, C. M. (2017). Observations from cyclic tests on deep, wide-flange beam-columns. *AISC Engineering Journal*. **54:1**, 45-61.

21. Palmer, K., Roeder, C., Lehman, D., Okazaki, T., and Shield, C. (2013). Experimental performance of steel braced frames subjected to bidirectional loading. *Journal of Structural Engineering*. **139:8**, 1274-1284.
22. PEER (2013). "The peer ground-motion selection web application." <http://ngawest2.berkeley.edu/>.
23. Richards, P. W., and Uang, C.-M. (2006). Testing protocol for short links in eccentrically braced frames. *Journal of Structural Engineering*. **132:8**.
24. Suita, K., Yamada, S., Tada, M., Kasai, K., Matsuoka, Y., and Shimada, Y. Collapse experiment on 4-story steel moment frame: Part 2 detail of collapse behavior. *Proc., 14th World Conference on Earthquake Engineering*, Beijing, China, 011.
25. Suzuki, Y., and Lignos, D. G. (2014). Development of loading protocols for experimental testing of steel columns subjected to combined high axial load and lateral drift demands near collapse. *Proc., 10th National Conference on Earthquake Engineering*, Anchorage, Alaska, USA.
26. Ucak, A., and Tsopelas, P. (2015). Load path effects in circular steel columns under bidirectional lateral cyclic loading. *Journal of Structural Engineering*. **141:5**.
27. USGS (2014). "Hazard curve application." <http://geohazards.usgs.gov/hazardtool/application.php>.
28. Watanabe, E., Sugiura, K., and Oyawa, W. O. (2000). Effects of multi-directional displacement paths on the cyclic behaviour of rectangular hollow steel columns. *J. Strutural Mechanics and Earthquake Engineering, JSCE*. **17:1**, 69-85.